DOI 10.7343/as-2024-701

ACQUE SOTTERRANEE
Italian Journal of Groundwater
journal homepage: https://www.acquesotterranee.net/

2024-AS48-701: 109 - 122

Integration of geoelectrical, hydrochemical and geothermal data to identify the origin of thermal water in the foothills of the Tlemcen mountains, Northwestern Algeria

Integrazione di dati geoelettrici, idrochimici e geotermici per identificare l'origine dell'acqua termale ai piedi dei monti Tlemcen, Algeria nord-occidentale

YOUSFI Somia[a] ✉ , **KERZABI Rachid**[a], **MUDRY Jacques**[b], **BENSALAH Mustapha**[a], **ACHACHI Aabdelhamid**[c], **COLLIGNON Bernard**[d]

[a] Laboratoire n°25 « PRHPM-LE-CT », Université de Tlemcen - Algérie - email ✉ : *sou.yousfi@gmail.com*
[b] Université de Franche-Comté, CNRS, Chrono-environnement, F-25000 Besançon, France.
[c] Agence Nationale de la Ressource Hydrique Oran- Algérie.
[d] Bottombillion, Avignon - France

ARTICLE INFO

Ricevuto/*Received*: 11 July 2023
Accettato/*Accepted*: 22 March 2024
Pubblicato online/*Published online*:
27 March 2024

Handling Editor:
Antonio Menghini

Citation:
Yousfi, S., Kerzabi, R., Mudry, J, Bensalah, M., Achachi, A., Collignon, B. (2024). Integration of geoelectrical, hydrochemical and geothermal data to identify the origin of thermal water in the foothills of the Tlemcen mountains, Northwestern Algeria. Acque Sotterranee - *Italian Journal of Groundwater*, 13(1), 109 - 122
https://doi.org/10.7343/as-2024-701

Correspondence to:
Yousfi Somia ✉
sou.yousfi@gmail.com

Keywords: *geophysics, geochemistry, Miocene basin, PCA, Remchi Plain, thermal water.*

Parole chiave: geofisica, geochimica, Bacino del Miocene, PCA, piana di Remchi, acqua termale.

Riassunto

In precedenti studi, il gradiente geotermico medio della regione di Tlemcen è stato stimato essere basso (3,7°C/100m). I pozzi trivellati nella piana di Remchi (a Nord delle montagne di Tlemcen) rivelano la presenza di acque termali (26-48°C) e un notevole artesianismo. Per comprendere l'idrodinamica e l'origine del termalismo di queste acque sotterranee, abbiamo analizzato congiuntamente i dati geofisici e i parametri fisico-chimici; i dati geofisici ci hanno permesso di migliorare la risoluzione della rete di faglie, di stimare lo spessore dei vari letti di arenaria connessi con il serbatoio idrotermale e di delimitare l'acquifero produttivo. Le caratteristiche chimiche delle acque sono state utilizzate per un'analisi statistica che ha mostrato la presenza di due cluster di acque indipendenti derivanti da due comportamenti idrodinamici nell'acquifero. L'analisi idrotermale ha identificato la profondità raggiunta dalle acque e la relazione tra la circolazione idrica e la rete di faglie. Il confronto con gli studi precedenti ha permesso di realizzare un modello geologico schematico, che spiega l'idrodinamica, l'origine e il ruolo di questa struttura nel flusso delle acque sotterranee.

Abstract

In previous studies, the mean geothermal gradient of the Tlemcen region has been estimated as low (3.7°C/100m). The existing boreholes in the Remchi plain (North of the Tlemcen Mountains) reveal thermal waters (26-48 °C) and a remarkable artesianism. To understand the hydrodynamics and origin of thermalism of this groundwater, we merged geophysical and physical-chemical data. Geophysical data allowed us to improve the resolution of the fault network, to estimate the thickness of various sandstone beds connected with the thermal reservoir and to delimit the productive aquifer. Chemical characteristics of waters have been used for a statistical analysis, which displayed two independent water clusters resulting from two hydrodynamic patterns throughout the aquifer. The hydrothermal analysis identifies the depth reached by water and the relationship between water circulation and the fault network. Comparison with previous studies allowed us to build a schematic geological model, which explains hydrodynamics, origin and role of this structure in the groundwater flow.

Introduction

Algerian thermomineral springs were inventoried and studied by many researchers as early as 1842. Several recent scientific works, dealing with regional thermal waters in Algeria (Issaadi 1996, 2005; Kedaid, 2006; Fekraoui, 2007; Ouali et al., 2007, Mansour et al. 2011, Bouchareb-Haouchine et al., 2012, Boudoukha et al., 2015 and Lakrout 2022) show that the geothermal Algerian resources are of low energy type, i.e. with temperatures lower than 90°C (BRGM, 2005). In the Carbonate Mountains of Tlemcen (NW Algeria), previous hydrogeological and geothermal studies estimated the mean geothermal gradient as 3.7 °C / 100 m (Collignon, 1986). However, recent exploitation of the Remchi plain sandstone aquifer, in the northern foothills, reveals remarkable thermal waters and artesianism. In the present work, we try to explain flow processes and groundwater origin, to better define the boundaries of the geothermal reservoirs in the Remchi plain, using the joint use of geological, structural, geophysical, hydrochemical and geothermal data.

The geoelectric method is considered an effective tool for mapping groundwater resources and identifying aquifer geometry. The mapping of horizontal and vertical variation of resistivity and the use of lithology maps, allowed us to determine the fault network and to identify three zones characterised by different depths and thicknesses of sandstone layers. In addition, we used Piper-Kelly and Duvor's diagram to determine the chemical facies and eventual water groups. However, understanding the origin of groundwater requires the statistical treatment of chemical samples.

Materials and Methods

Study area

The study area is located in the North West of Algeria and occupies the Northern foothills of the Tlemcen Mountains (Western part of the Tell Atlas); it is limited to the North by the Sebâa Chioukh ridge, to the East by the Isser wadi, and to the West by the Tafna wadi.

Located in the middle of Tafna, the study area is covered by the watersheds of Boumessaoud, Zitoun, Sikkak and Isser wadis (Fig. 1), all originated from the Jurassic formations of the Tlemcen Mountains. It joins the Tafna wadi towards the North, crossing the Remchi plain.

The climatic regime in this area is similar to that of the semiarid Mediterranean areas of Northern Algeria (Meddi et al., 2010). The precipitations range from 160 to 1100 mm/year, as observed in ten weather stations of the middle Tafna watershed (Belarbi, 2018; Amar Belarbi & Bensliman, 2023).

Geological and hydrogeological setting

The Tlemcen Mountains and their Northern foothills are characterised by two geological domains: the karstic Jurassic carbonate massif and the Miocene formations filling the large northern basin (Fig. 2). The first domain includes three main aquifers (Bensaoula, 2007), from the bottom to the top:

- Boumedien sandstone aquifer: 500m of moderately pored and fissured sandstones;
- Lower member: dolomitic limestone formations, 200 to 300 m thick;
- and the Upper member: dolomitic limestone formations, 120 to 150 m thick.

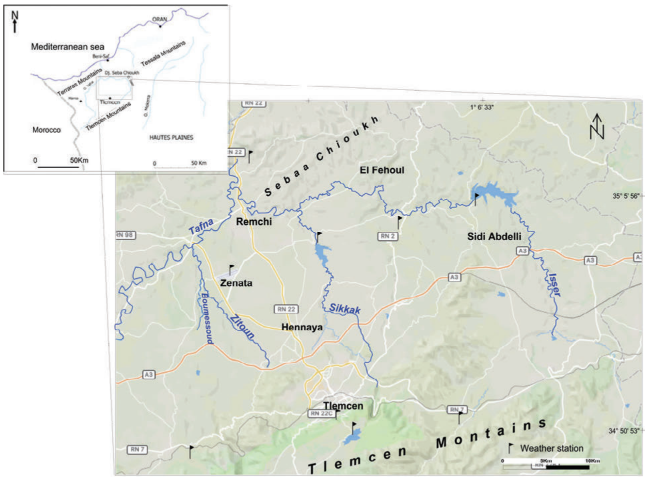

Fig. 1 - Geomorphological map of the study area (topographic base from mapcarta.com).
Fig. 1 - Carta geomorfologica dell'area studiata (base topografica da mapcarta.com.

The second one is characterised by marl with sandstone intercalations, dating from the Serravallian, and sandstone formations dating from the Tortonian. To illustrate this, we used a lithostratigraphic detailed description of the principal units of the ara (Clair, 1974; Guardia, 1975 and 1984; Benest et al., 1999; Bensaoula, 2007 and Kerzabi, 2008), togther with a hydrogeological description (Fig. 3). Only the Jurassic formations can form significant groundwater reservoirs. However, several geoelectric prospections (ENAGEO, 1979; 1983; 1987; ICOSIUM, 2002) have identified resistive layers in the Remchi plain that are associated to the Serravalian aquifer (Fig. 4), which provides a cumulative flow of 25 to 140 L/s.

Geoelectrical data acquisition

The geological structure of North of Algeria plays a major role in the occurrence of thermal springs; the majority of thermal springs in the centre of Algeria are favoured by faults oriented NE-SW, NW-SE, EW (Nedjaï, 1987). This occurs also in Western Algeria, where the faults oriented NE-SW are connected with many thermal springs (Fekraoui, 2007). Thus, a structural overview of the Tlemcen region becomes useful to understand the thermal behaviour of groundwater.

The Tlemcen Mountains are affected by a succession of horsts and grabens oriented N50° to N70°. They are limited by normal faults, whose displacement reaches at least 500m (Collignon, 1986). There is an important system of subvertically dipping fractures, either longitudinal SW-NE to WSW-ENE (corresponding with the most frequent Tellian trend) or oblique with transverse faults N-S to NNE-SSW (Benest et al., 1999).

The recent use of geophysics (ICOSIUM, 2002) shows the existence of an important resistive formation that can be characterised by high hydraulic conductivity. This is why we carried out a geoelectric prospecting campaign. Conventional

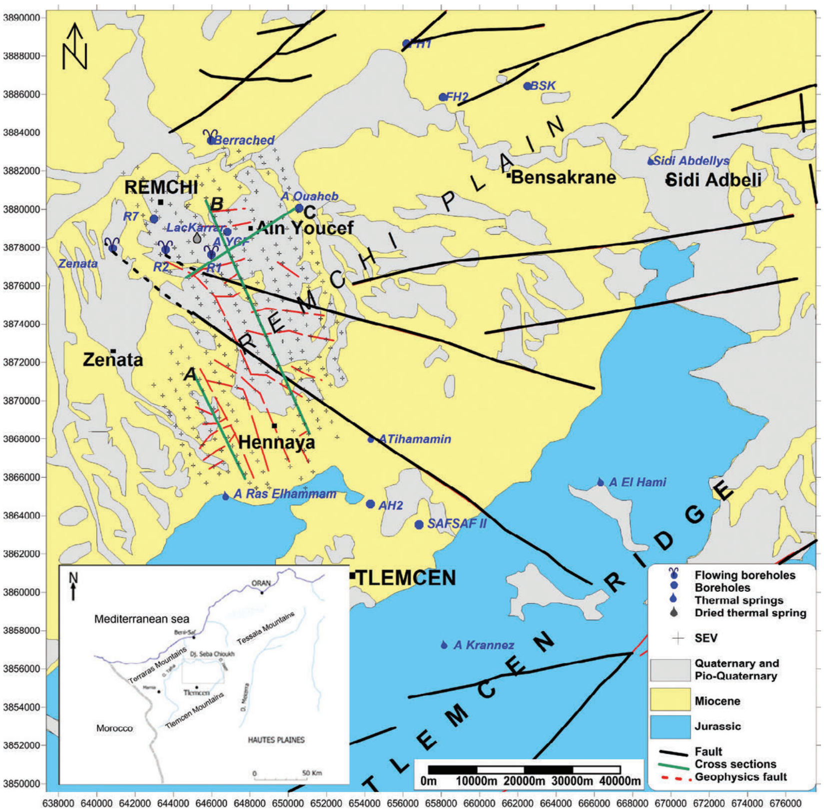

Fig. 2 - Geostuctural map of the Tlemcen Mountains and the Remchi plain (ANRH, 2008, simplified).

Fig. 2 - Carta geostrutturale dei Monti Tlemcen e della Piana di Remchi (ANRH, 2008, semplificata).

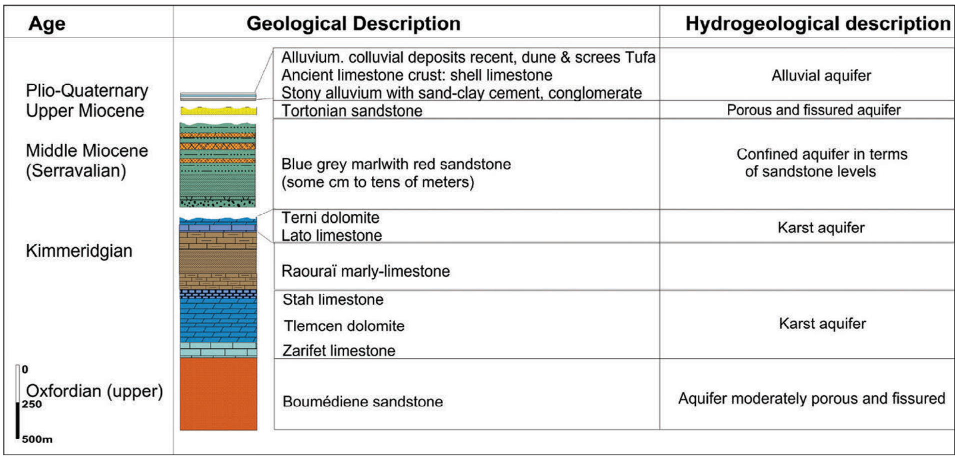

Age	Geological Description	Hydrogeological description
Plio-Quaternary	Alluvium. colluvial deposits recent, dune & screes Tufa Ancient limestone crust: shell limestone Stony alluvium with sand-clay cement, conglomerate	Alluvial aquifer
Upper Miocene	Tortonian sandstone	Porous and fissured aquifer
Middle Miocene (Serravalian)	Blue grey marlwith red sandstone (some cm to tens of meters)	Confined aquifer in terms of sandstone levels
Kimmeridgian	Terni dolomite Lato limestone	Karst aquifer
	Raouraï marly-limestone	
	Stah limestone Tlemcen dolomite Zarifet limestone	Karst aquifer
Oxfordian (upper)	Boumédiene sandstone	Aquifer moderately porous and fissured

Fig. 3 - Lithostratigraphic and hydrogeological log.

Fig. 3 - Log litostratigrafici e idrogeologici.

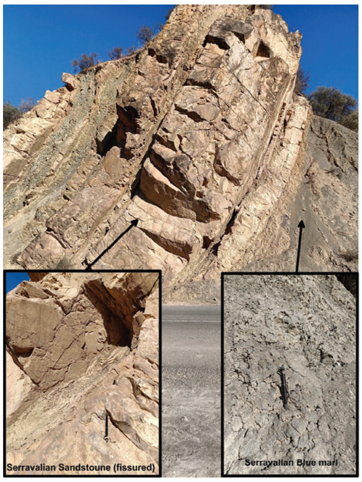

Fig. 4 - Outcrops of Serravalian formation in Sebaa Chioukh Mountains.

Fig. 4 - Affioramento della Formazione Serravalliana nelle Montagne di Sebaa Chioukh.

Schlumberger array (Fig. 5) (Telford et al., 1990) was used to perform 317 vertical electrical soundings (VES) (located in Fig. 2), with the electrode spacing (AB) being extended to a maximum of 4000 m in some of the sites. This study uses resistivity calibration values (Tab. 1), obtained both by in situ measurements near the formation outcrops, and by comparison with existing boreholes lithostratigraphic information (8 boreholes, with depth varying between 90 and 600 m). Figure 6 presents the results of modelled curve types in the following sites: Hennaya, Karrar, Zenata, Ain Youcef, Sid M'barek, RMC1, RMC2 and Berrached. This was represented by the apparent resistivity curve, the forward model and the relative 1D resistivity model.

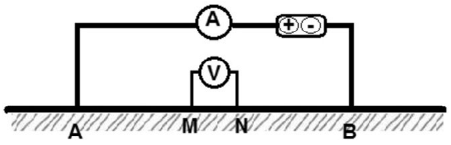

Fig. 5 - Schlumberger electrode configuration.

Fig. 5 - Configurazione degli elettrodi Schlumberger.

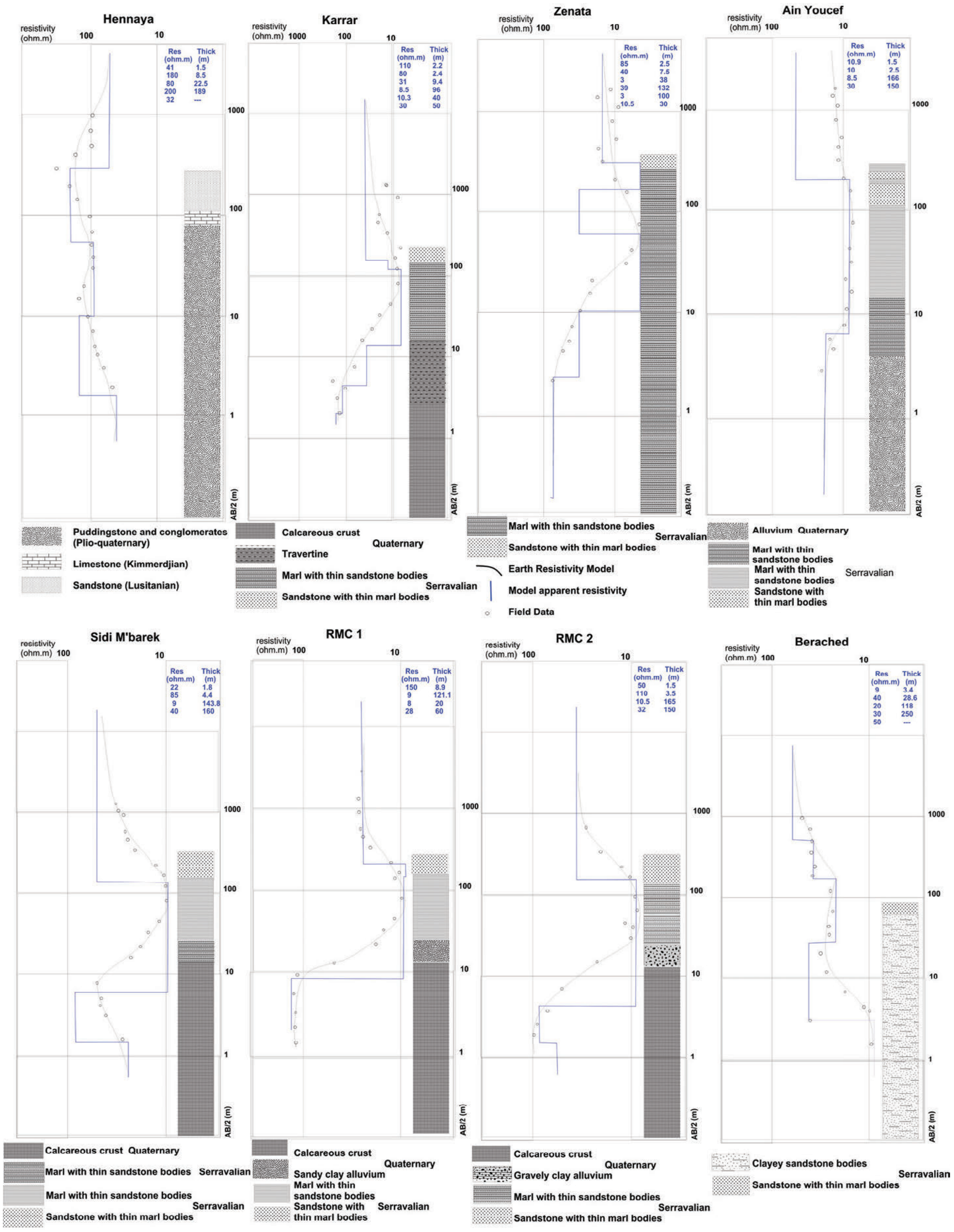

Fig. 6 - Calibration of VES with boreholes lithostratigraphic column (ICOSIUM, 2002).

Fig. 6 - Calibrazione di VES con i logs stratigrafici (ICOSIUM, 2002).

Tab. 1 - Calibration values of resistivity (ICOSIUM 2002).

Tab. 1 - Valori di calibrazione della resistività (ICOSIUM 2002).

Formations	Resistivity (Ohm-m)	Age
Alluvium	10-280	Quaternary
Calcareous crust	23-210	
Travertine	31-480	
Pudding stone, conglomerate and sandstone	42-150	Plio-Quaternary
Yellow clay with sandstone bodies	10	
Blue marl	2-9	Miocene (Serravalian)
Blue marl with thin sandstone bodies	9-16	
Sandstone with thin marl bodies	19-77	
Limestone et dolomitic formations	90-700	Jurassic (Kimmeridgian)

Hydrochemical data acquisition

As part of a monitoring of the water quality of the Remchi plain, the ANRH in collaboration with the ADE (Algérienne Des Eaux) carried out a sampling campaign in March 2015 on 11 boreholes and Sidi Abdellys spring (Fig. 7). All boreholes capture the Serravalian sandstone aquifer. Temperatures and pH were measured in situ. The sample was kept cold and stored in 1.5 litre polyethylene bottles. The chemical characteristics (Cl^-, Ca^{2+}, Mg^{2+}, K^+, Na^+, SO_4^{2-}, HCO_3^-, and NO_3^-) were measured in the laboratory according to the analysis methods recommended by Rodier (2009). We used only the physico-chemical analyses with ionic balance values better than ±5 %. The temperatures of the outflowing waters in the study boreholes are mapped in Figure 7.

Results and Discussions

Geoelectrical study

We have processed and interpreted the geoelectric data and achieved all geoelectric profiles in order to locate any anomaly in resistivity variation. These anomalies, representing faults detected by geophysical prospection, are plotted on the geological map (Fig. 2).

The combination of geoelectric cross-sections, surface and subsurface geological data (Fig. 8) allowed us to recognize three zones:

1. in the South of the Remchi plain, Miocene sandstone formations are frequent and shallow. They are in contact with the Jurassic formations (Fig. 8- A);

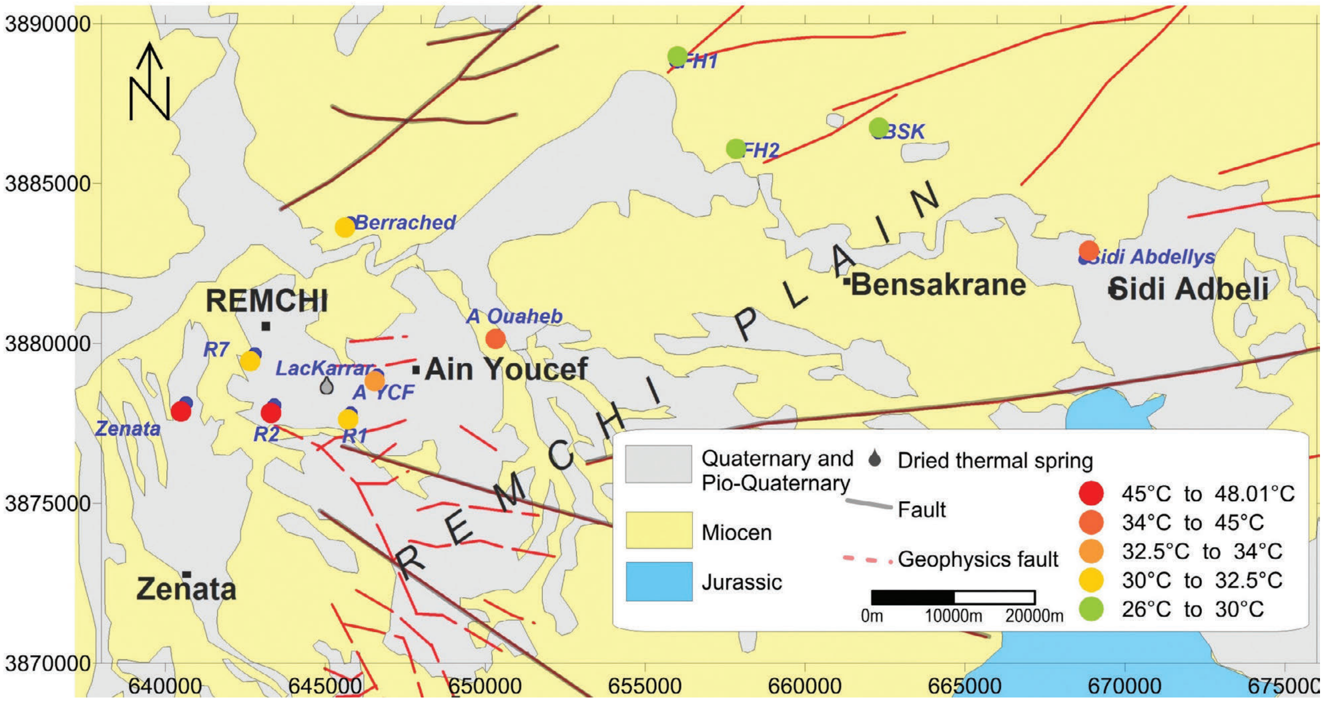

Fig. 7 - Sampling map showing the spatial water temperature variability of thermal boreholes and spring in the Remchi plain.

Fig. 7 - Carta di campionamento che mostra la variabilità spaziale della temperatura dell'acqua dei pozzi termali e delle sorgenti nella pianura di Remchi

2. in the centre of the Remchi plain, Miocene sandstone formations are absent at depths lower than 450 m. This zone constitutes a waterproof section which isolates laterally the third zone from the Tlemcen Mountains (Fig. 8- B):
3. in the Northern zone, the sandstone formations constitute thick layers with depths ranging between 50 and 300m. They constitute a deep aquifer with significant hydraulic potentiality (Fig. 8-C).

The isoresistivity maps show the lateral and vertical variation of the apparent resistivity in the study area for five depth slices (Fig. 9). The analysis of the apparent resistivity map AB=200 m allowed us to distinguish the following areas: a) high resistive area in the South, corresponding to Jurassic outcrops; b) intermediate resistive area in the center, occupying by the Pudding stone, conglomerate of Plio-Quaternary; c) the rest of the map is occupied by low resistivity, corresponding to Serravalian marls.

With AB spacing between 600 and 2000 m, the distribution of apparent resistivity highlights two zones (1 and 3 in Fig. 8B) that correspond well to the sandstone with thin marl layers. Resistivity values lower than 20 ohm-m characterise the center part of the map and some part of the northern west, which corresponds to the area occupied by the Serravalian conductive level (zone 2 in Fig. 8B).

The map for the last layer resistivity (AB 4000m) specifies a low resistivity in the northern part of the study area; these values might be due to the absence of sandstone layers at great depth.

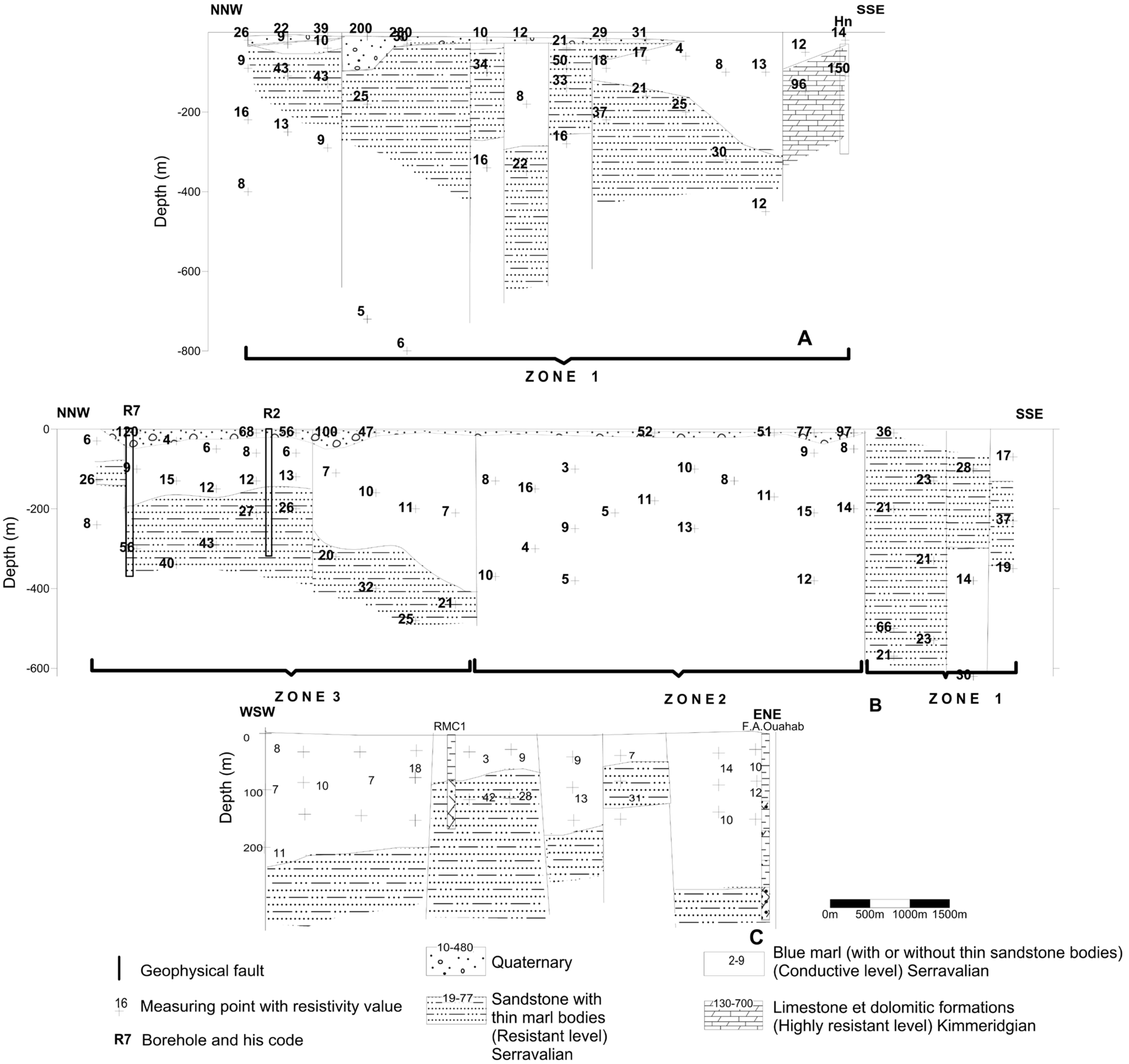

Fig. 8 - Geoelectric cross-sections.

Fig. 8 - Sezioni geoelettriche.

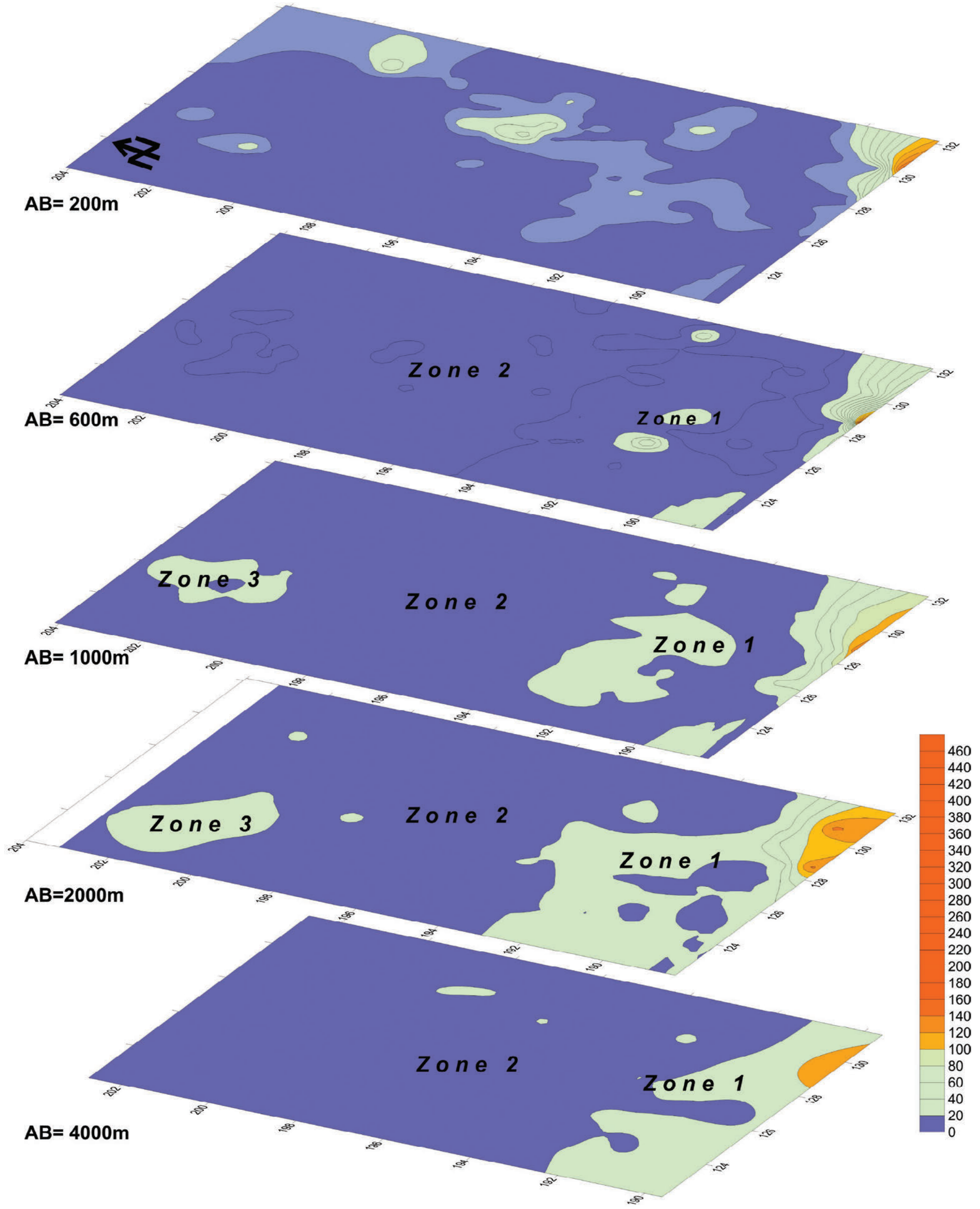

Fig. 9 - Isoresistivity maps for different AB.

Fig. 9 - Carte di isoresistività per diversi AB.

Hydrochemical study

A Piper-Kelly diagram is used to characterise the groundwater geochemistry through the identification of water type. Seven distinct grading criteria were employed, from freshwater to conservative mixing water, to characterise the seawater intrusion (Zamroni et al., 2021; Gueddari et al., 2022) or salt-water encroachment from the Sebkha (Mhamdi et al., 2022).

Clustering Remchi plain groundwater samples in the Kelly diagram (Fig. 10) shows that Cl-SO_4/Na–Ca is the dominant water facies. In general, the abundance of anions displays a Cl (40-80%)> SO_4 (20-60%)> HCO_3 (10-50%) evolution. While the abundance of cations displays a Na^+K (47–85%) > Ca (15–55%) > Mg (8–40%) evolution.

The knowledge of the chemical characteristics was used to investigate the origin of salinity in the aquifer (Dazy et al., 1987; Bianchetti et al., 1992; Abdesselam et al., 2000; Khaska et al., 2013 and Saberinasr et al., 2019). The groundwater samples from the Serravalian aquifer reveal the chloride type of groundwater; this is probably the result of exchanges with Triassic formations, which constitute the first source of chloride ions. However, the latter are unknown as outcrops in the Tlemcen Mountains (Collignon, 1986). The acquisition of sulphate could be accounted by for the dissolution of gypsum which is present in the lower marls of the Miocene. It also indicates that the thermal waters have a deep flow and a calcareous recharge area origin (HCO_3^- concentration). The content of ^{18}O at Lake Karar shows that the recharge area is quite high, probably the Tlemcen mountains (Collignon, 1986). S. Abdellys spring is the only one displaying the bicarbonate type. It suggests that this aquifer is made of Jurassic carbonate rocks.

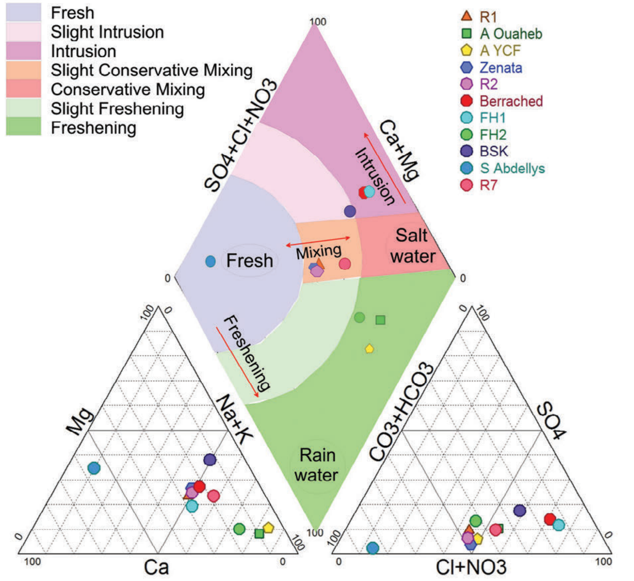

Fig. 10 - Piper–Kelly diagram of the Remchi plain water samples.

Fig. 10 - Diagramma Piper-Kelly dei campioni di acqua della pianura di Remchi.

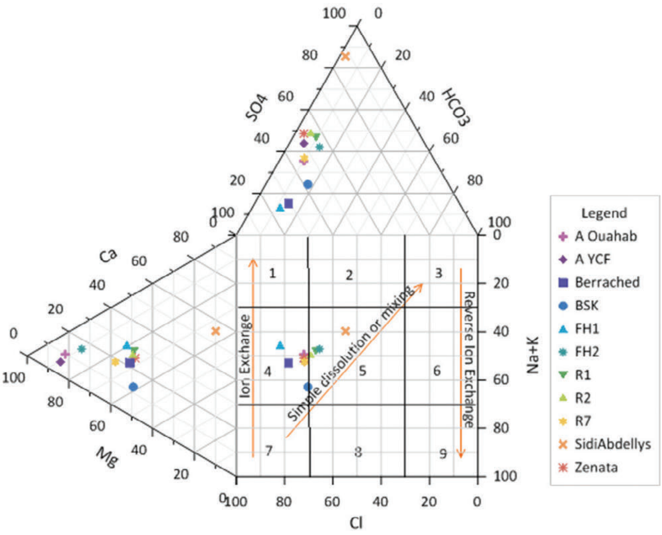

Fig. 11 - Durov plot illustrating hydrochemical processes involved in groundwater in study area.

Fig. 11 - Grafico di Durov che illustra i processi idrochimici coinvolti nelle acque sotterranee nell'area di studio.

Durov diagram has been used to identify hydrochemical processes in groundwater, classifying different types of water mixing, the presence of ions, and reverse ion exchange processes. The geochemical processes occurring in the groundwater of the study area were further verified by Durov's plot (Fig. 11). It showed that the groundwater samples are plotted in fields 4 and 5. The fitting of samples in field 4 showed the occurrence of Ca^{2+} and SO_4^{2-} as the dominant ions in the water, and they are mainly due to the gypsum dissolution process. Some samples are plotted in field 5, which indicates that water exhibits simple dissolution or mixing occurring between two or more different facies (no dominant cation or anion) (Lloyd & Heathcoat, 1985). The recent study in the Hennaya plain (Plio-quaternary aquifer) (Yebdri, 2023) showed that 98% of samples belong to group 5. These waters are considered as mixed water, which confirms that they are mixed with a recent freshwater recharge, highlighting the contribution of the Northern recharge area (Sebâa Chioukh Mountains) to the aquifer recharge.

Statistical analysis

Correlation analysis

Bivariate correlation technique is initially applied as the first assessment of the hydrochemical origin of the facies. Admitting that for 10 degrees of freedom, a correlation factor $R^2 > 0.815$ implies a statistically significant degree of correlation, Table 2 displays a good correlation between Ca^{2+}, Mg^{2+}, Na^+ and Cl^-, SO_4^{2-}, suggesting that most elements have an evaporite origin.

Principal Component Analysis (PCA)

Principal Component Analysis is largely used to analyse hydrochemical data of karst aquifers (Bakalowicz, 1979; Blavoux & Mudry, 1986; Razack & Dazy, 1990 and Hamit,

Tab. 2 - Pearson correlation matrix for Serravalian aquifer parameters in the Remchi plain.

Tab. 2 - Matrice di correlazione di Pearson per i parametri dell'acquifero serravaliano nella pianura di Remchi.

Variables	Ca	Mg	K	Na	Cl	SO_4	HCO_3	NO_3
Ca	1							
Mg	0.672	1						
K	-0.226	0.411	1					
Na	0.498	0.505	0.061	1				
Cl	0.842	0.781	0.063	0.856	1			
SO_4	0.689	0.866	0.312	0.819	0.914	1		
HCO_3	-0.295	-0.134	0.051	0.446	0.038	0.236	1	
NO_3	0.541	0.380	0.033	0.190	0.384	0.518	0.080	1

2012), and it is considered an efficient statistical tool to infer groundwater origin (Mudry 1987 and Marín Celestino 2018). It is applied to groundwater quality data to extract principal factors corresponding to the different sources of hydrochemistry variation (Helena et al., 2000; Mouser et al., 2005 and Belkhiri et al., 2010), and contamination sources (natural and anthropogenic; De Andrade et al., 2008), especially in semi-arid zones (Yousfi, 2014). PCA of the hydrochemical data will clearly define the element markers of the Miocene sandstone aquifer in the confined zone and the flow conditions of groundwater (Fig. 12). Eight hydrochemical variables were considered: Mg^{2+}, Ca^{2+}, K^{+}, Na^{+}, SO_4^{2-}, Cl^{-}, HCO_3^{-} and NO_3^{-}. Two factors (F1 and F2) explaining together 72% of total variance allowed us to classify the variables into two distinct groups (Fig. 12): the first cluster is defined by Mg^{2+}, Ca^{2+}, Na^{+}, SO_4^{2-}, Cl^{-} . Explaining 54% of the variance. These tracers explain the dissolution of Triassic formation in deep and evaporite rocks that are present in the basis of Miocene. HCO_3^{-} make alone the second group, with 18.13% of variance indicating a carbonate origin. This factor plan is typical of an evaporate-carbonate typical behaviour. Two tracers are poorly represented in the factor plan 1x2. K^{+}, which is generally typical of clayey media, defines alone F3, and NO_3^{-}, typical of anthropogenic origins, defines alone F4. The data set is highly dominated by halite and gypsum, two major minerals of evaporate contents.

The analysis of the projection for S. Abdellys spring and boreholes in the factor plane F1xF2 (Fig. 12) shows that the measurement points can be subdivided into three groups:

- The first group: characterised by strong mineralization in boreholes FH1 and Berrached (north of Remchi plain). This mineralization is connected to the lithology of the aquifer;
- The second group presents high rates of bicarbonate corresponds to the boreholes FH2, BSK, A. Ouahab and A. YCF. These boreholes are located along a fault, favouring upward circulation of deep bicarbonate waters.
- The third group: These are the least mineralized waters, compared to the other groups, Zenata, R7, R2, R1 and S. Abdellys.

Geothermal conditions

To estimate the depth of the deep aquifer, we calculated the thermal anomaly of the water according to Collignon (1986), by correcting the air and water temperatures. The results are presented in table 3, with a minimal depth reached by water ranging between 277 and 867 m. FH1, FH2 and BSK are characterised the lower values, where the sandstone formation is shallower. In the West (Zenata and R2), water temperature is 45 and 48°C, respectively, which can be due to a deeper aquifer and a rapid water rise favoured by faults. The rising waters at 31°C feeding Lake Karar (currently dry) showed a similar context of emergence (Fig. 13), favoured by a fault. This can be explained by the three boreholes, heavily mineralized with bicarbonates (A. Ouaheb, FH2, A. YCF and BSK) which are aligned and located near a geological fault which should cross Lake Karar. Around this spring, we can clearly distinguish a travertine massif (3 km²) with a few tens of meters of thickness. At the core of this massif, mesothermal water emerges. This basin existed until the beginning of the 20th century, but its age can be dated from the Middle Pleistocene.

The relationship between thermal anomaly and the mean screen depth (Fig. 14) presents a linear correlation, displaying a geothermal gradient of 4.8°C/100m, that agrees with

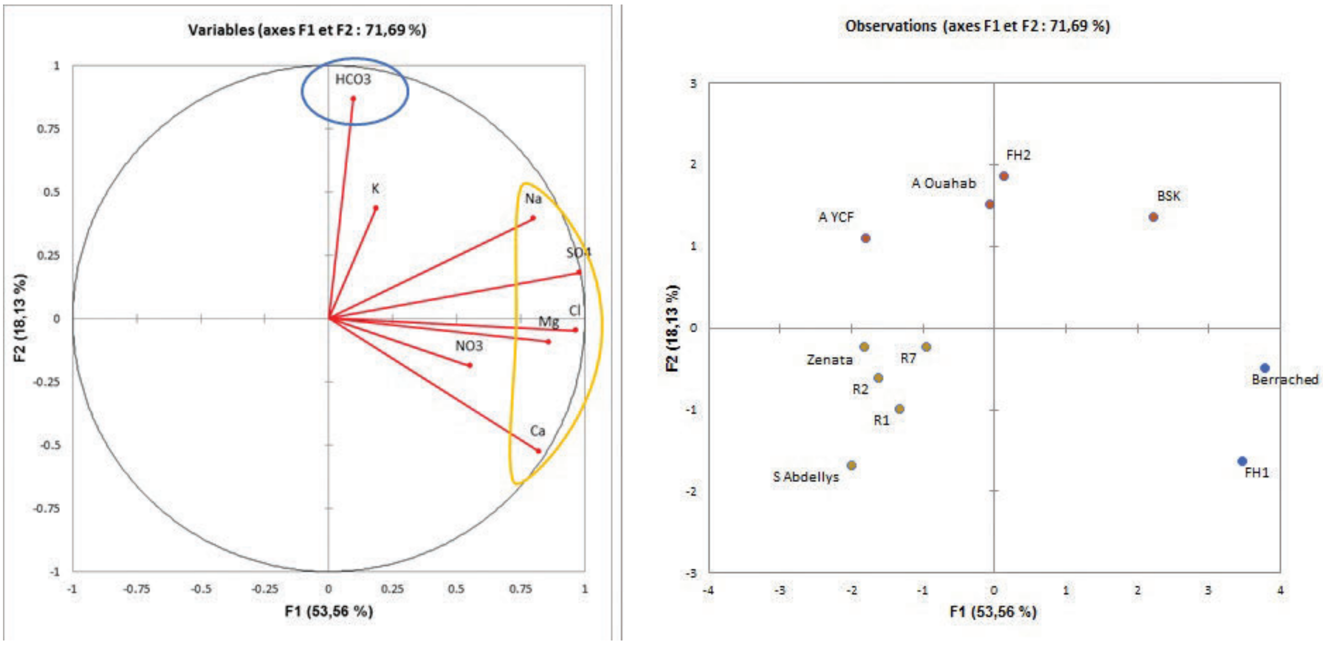

Fig. 12 - Correlation between chemical parameters and factors F.

Fig. 12 - Correlazione tra parametri chimici e fattori F.

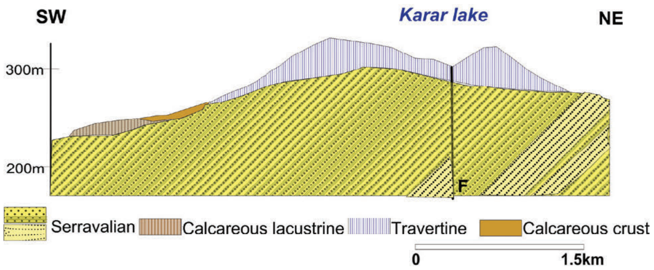

Fig. 13 - Geological cross section of Karar Lake .

Fig. 13 - Sezione geologica del Lago Karar.

the calculated one in the Oran meseta region (Blavoux & Collignon, 1986).

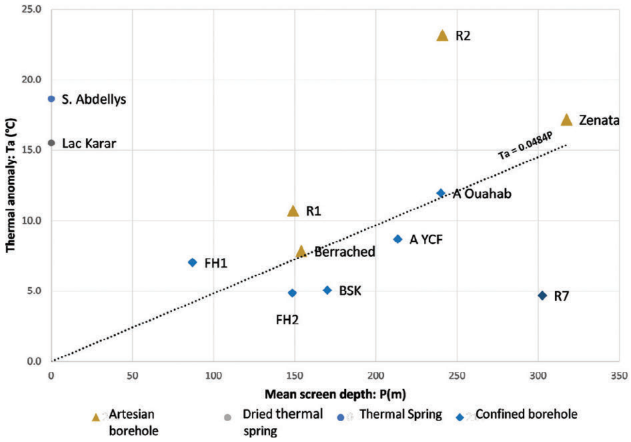

Fig. 14 - Thermal anomaly vs. mean screen depth.

Fig. 14 - Anomalia termale vs. profondità media dei filtri.

Tab. 3 - Boreholes characteristics.

Tab. 3 - Caratteristiche dei pozzi.

Location	Alt (asl)	Correction of altitude (Z*0.55/100)	Tair= 17.29- Calt	Water Temperature Tw (asl)	Mean screen depth (P)	Expected temperature (asl)	Thermal anomaly Tw-Tair	Estimated depth of the deep aquifer
	m	Calt	°C	°C	m	Tair+P*0.037	°C	m
R2	248	1.4	15.9	48	241	24.8	23.2	867
Zenata	219	1.2	16.1	45	318	27.8	17.2	781
A Ouahab	203	1.1	16.2	37	240	25.1	11.9	563
S. Abdellys	350	1.9	15.4	34	0	15.4	18.6	504
A YCF	250	1.4	15.9	32.5	214	23.8	8.7	448
R1	275	1.5	15.8	32	149	21.3	10.7	438
R7	210	1.2	16.1	32	303	27.3	4.7	429
Lac Karar	327	1.8	15.5	31	0	15.5	15.5	419
Berrached	150	0.8	16.5	30	154	22.2	7.8	366
BSK	480	2.6	14.7	26	170	20.9	5.1	307
FH2	300	1.7	15.6	26	149	21.1	4.9	280
FH1	280	1.5	15.8	26	87	19.0	7.0	277

Hydrogeological model

Geoelectric cross-sections, in combination with surface geological data and hydrochemical analyses, allowed us to build a conceptual hydrogeological model of groundwater flow from recharge zones of the Tlemcen Mountains to the thermal aquifer (Fig. 15).

This cross-section was realised by the projection of outcropping formations in the Tlemcen sheet of the geological maps (1/50,000), boreholes, lithostratigraphic column, and geophysics information (faults and location of sandstone formations), in order to complete the knowledge about geological setting and the regional groundwater flow. We identify three zones: the first, where the sandstone formations are in contact with Jurassic formations of the Tlemcen Mountains, which take part in lateral water inflow. The second zone is characterised by the absence of sandstone formations at more than 450 m depth. The third zone represents the confined thermal sandstone aquifer. The structure of this zone plays an important role for vertical water inflow in the West of the Remchi Plain (Zenata, R7, R2, etc.); there is an increasing depth of the sandstone aquifer in the East, where the water temperature is low (FH1, FH2, Berrached).

Physical-chemical analyses help us to understand the hydrodynamic behaviour of groundwater. The thermal water in Remchi plain spends a long time in the sandstone formations, explained by a substantial vertical path in the South, from the Jurassic recharge area to the aquifer, deeper than 450 m. The hypothesis of halite dissolution from deeper Triassic formation could explain the origin of chloride concentrations in the Remchi plain groundwater. The limestone outcrops of Jurassic formations are the principal recharge area of the thermal aquifer, which provides bicarbonates in all water samples. In addition, the proportional relationship between water temperature and depth of the aquifer top corroborates the above-mentioned results.

The flow map of the Tlemcen Mountains (Fig. 16) shows

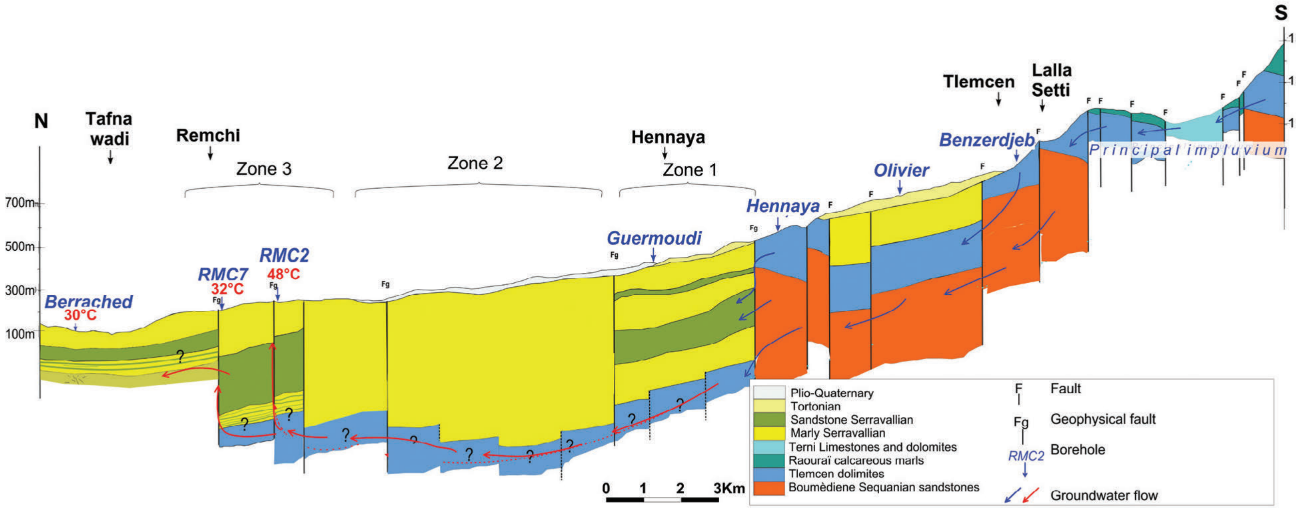

Fig. 15 - Hydrogeological model of groundwater.

Fig. 15 - Modello idrogeologico delle acque sotterranee.

that the main direction of flows in the Northern foothills is towards units buried under the Miocene formation. The aquifer system extends under low permeable or impermeable cover; there are piezometric indicators to specify the flow direction. This map can explain artesian flow in Remchi Plain.

Conclusions

Multi-criteria analyses of data about the deeper aquifer in Remchi plain, show the important relationship between water circulation and physical-chemical parameters; in this study case, the high temperature of water is explained by a significant path to the aquifer, deeper than 450 m. The interpretation of the different geological sections as well as all the apparent isoresistivity maps allowed us to identify the geometry of Serravalian sandstone-marl layers. We have a better understanding of vertical and lateral hydraulic connections between sandstone or marly sandstone aquifers and Jurassic dolomitic limestone formations.

Geospatial analysis of hydrochemical parameters indicated spatial variation and heterogeneities in water quality analyses. In the study area, heat water ascent is caused by normal faults crossing the plain to the SW and NE. This water has a deep path, contributing to its mineralization. The Miocene marls can be the origin of high concentrations of gypsum elements, whereas the halite elements indicate that sulphates are likely

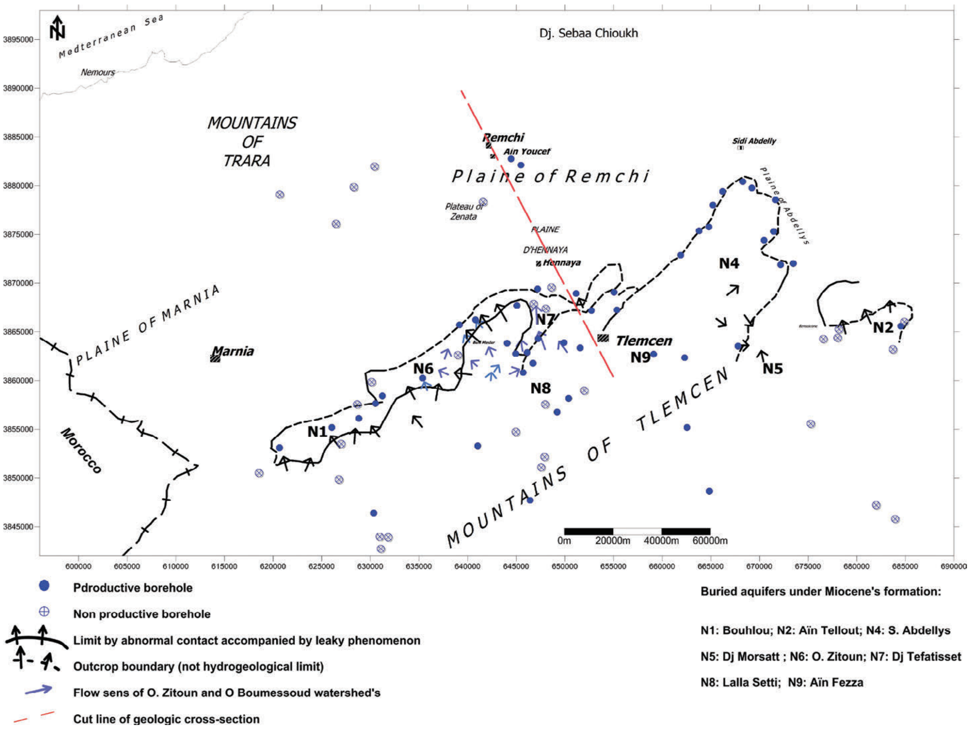

Fig. 16 - Flows of karst aquifers (Northern foothills of Tlemcen mountains) (ANRH, 1995 modifed).

Fig. 16 - Flusso degli acquiferi carsici (versante settentrionale ai piedi dei monti Tlemcen) (ANRH, modificato nel 1995).

to originate from dissolution within Triassic formations. Some studies have been conducted on the groundwater quality of 50 water points in the northern foothills of the Tlemcen Mountains: O. Zitoun and O. Boumessoud (Touati & Nebia, 2019), Sabra and Béni Senous (Boukacem & Derbal, 2019) and Tlemcen Urban Group (Amar Belarbi & Benslimane, 2023) show that nitrate concentrations range from 12 to 98 mg/L (Beni Mester2). We deduce that the shallow location of these waters favours contamination by fertilizers and/or discharges of urban wastewater, while the low nitrate content in the Remchi plain waters (less than 10 mg/L) can be explained by a deeper origin.

It should also be noted that the thermal waters of the Zouia deep Liassic aquifer (Western foothills of the Tlemcen Mountains) have Sodium bicarbonate, Sodium chloride and Sodium sulphate facies (Bensaoula et al., 2005; Bensaoula & Adjim, 2006; Benkhlifa & Lamouri, 2018). The origin of chlorides and sodium may be the leaching from Triassic formations (Bensaoula & Adjim, 2006).

The results yielded by this survey show the necessity of preparing a more detailed study (isotopic analyses), which should help in exploiting this thermal aquifer.

The hydrogeological model built in this study, based on geological, hydrogeological and geophysical information, identified the extension of the thermal aquifer and explained the groundwater circulation from the Jurassic recharge zone to the sandstone aquifer.

Competing interest

All authors, declare no competing interests.

Author contributions

Collection of data and interpretation of results, Rachid Kerzabi and Abelhamid Achachi; data processing, interpretation of results and writing-original draft preparation, Somia Yousfi; visualization and supervision, Jacques Mudry, Mustapha Bensalah and Bernard Collignon.

All authors have read and agreed to the final version of the manuscript.

Additional information

DOI: https://doi.org/10.7343/as-2024-701

Reprint and permission information are available writing to acquesotterranee@anipapozzi.it

REFERENCES

Abdesselam M., Mania J., Mudry J., Gelard J.-P., Chauve P., Lami H. & Aigoun C. (2000). Argument hydrogéochimique en faveur de Trias évaporitique non affleurant dans le massif du Djurdjura (dorsale kabyle, élément des Magrébides), *Hydrogeochemical argument in favor of evaporitic Trias not outcropping in the Djurdjura massif (Kabyle ridge, Magrébides element)*, Revue des Sciences de l'Eau, 13/2, 155-166.

Amar Belarbi Y. & Bensliman M. (2023). Etude hydrogéologique et caractérisation spatio-temporelle de la qualité des eaux souterraines du groupe urbain de Tlemcen. *Hydrogeological study and spatio-temporal characterization of groundwater quality in the urban group of Tlemcen.* Master thesis, University of Tlemcen 140 p.

ANRH (1995). Map of the Tlemcen Mountains Large Karst Aquifers (1/200 000).

Bakalowicz M. (1979). Contribution à l'étude de la géochimie à la connaissance de l'aquifère Karstique et de la Karstification, *Contribution to the geochemistry study to the knowledge of the Karst aquifer and Karstification*, Thesis Sciences, Paris Sud, Orsay, 275p.

Belarbi F. (2018). Etude des précipitations, du transport solide dans le bassin versant de la Tafna et leur interrelation. *Study of precipitation, solid transport in the Tafna watershed and their interrelationship.* Ph.D. thesis, University of Tlemcen, 185p.

Belkhiri L., Boudoukha A., Mouni L. & Baouz T. (2010). Multivariate statistical characterization of groundwater quality in Ain Azel plain, Algeria. Multivariate statistical characterization of groundwater quality in Ain Azel plain, Algeria, African Journal of Environmental Science and Technology, 4(8), 526-534.

Benest M., Bensalah M., Bouabdellah H. & Ouardas T. (1999). La couverture mésozoïque et cénozoïque du domaine Tlemcénien (Avant pays Tellien d'Algérie occidentale) : Stratigraphie, paléoenvironnement, dynamique sédimentaire et tecto-genèse alpine. *The Mesozoic and Cenozoic Cover of the Tlemcenian Domain (Tellien Foreland of Western Algeria): Stratigraphy, Paleoenvironment, Sedimentary Dynamics and Alpine Tectogenesis,* Bulletin of the Geological Survey of Algeria, , 10, 2.

Benkhlifa S. & Lamouri S. (2018). Contribution à l'étude hydrogéologique de la nappe du Bajo-Bathonien (Nord-Ouest Algérie). *Contribution to the hydrogeological study of the Bajo-Bathonian aquifer (North-West Algeria)*, Master's thesis, University of Tlemcen 80 p.

Bensaoula F. (2007). Etude de la karstification à partir des données de forage : le cas des Monts de Tlemcen (Algérie). *Study of karstification from borehole data: the case of the Tlemcen Mountains (Algeria)*, Karstologia, 49, 2007. 15-24.

Bensaoula F. & Adjim M. (2006). Synthèse sur les forages hydrauliques profonds de la zone frontalière algéro-marocaine. *Synthesis on deep hydraulic drilling in the Algerian-Moroccan border area,* Larhyss journal n°5, pp.33-48

Bensaoula F., Bensalah M. & Achachi A. (2005). Etude des circulations d'eaux profondes dans les dolomies du dogger de Zouia (bordure occidentale des Monts de Tlemcen, nord-ouest algérien. *Study of deep water circulations in the dolomites of the Zouia dogger (western edge of the Tlemcen Mountains, northwestern Algeria.* Hydrogeology Bulletin, 21, 17-31.

Bianchetti G., Roth P. & Vuataz F.-D. (1992). Deep groundwater circulation in the Alps: Relations between water infiltration, induced seismicity and thermal springs. The case of Val d'Illiez, Wallis, Switzerland, Eclogae Geologicae Helvetiae, 85, 2, 291-305.

Blavoux B. & Mudry J. (1986). Influence des pluies estivales sur la qualité des réserves de l'aquifère karstique : le rôle du sol et de l'épikarst dans la concentration des chlorures. *Influence of summer rains on the quality of karst aquifer reserves: the role of soil and epikarst in chloride concentration*, Bulletin de la Société Géologique de la France, 11, 4, 667-674.

Blavoux B. & Collignon B. (1986). Les Sources Bicarbonatees Thermales des piemonts de la Meseta Oranaise. *The Bicarbonate Thermal Springs of the foothills of the Meseta Oranaise*, 6th National Seminar on Earth Sciences (Algiers December 1986)

Boudoukha A., Athamna M. & Benaabidate L. (2015). Etude du potentiel hydrothermal de hammam Sokhna. Est algerien. *Study of the hydrothermal potential of Sokhna hammam East of Algeria*, Larhyss Journal, ISSN 1112-3680, 24, Decembre 2015, 161-174.

Boukacem K. & Derbal F. Z. (2019). Etude hydrochimique et qualitative des eaux souterraines des régions de Béni Snous et Sabra (N - O algérien). *Hydrochemical and qualitative study of groundwater in the regions of Beni Snous and Sabra (N.W. Algeria).* Master's thesis, University of Tlemcen 76p.

BRGM (2005). Géothermie très basse et basse énergie : Une énergie du développement durable. *An energy of sustainable development. Scientific summary sheet*, BRGM, Orléans, 5 p.

Clair A. (1974). Rénovation rurale, aménagement de la région de Tlemcen. Rapport de synthèse (cartes et notices). *Rural renewal, development of the Tlemcen region. Synthesis report (maps and notices),* Record of the lithological map of the region of Tlemcen at 1/100.000. SODETEC.

Collignon B. (1986). Hydrogéologie appliquée des aquifères karstiques des Monts de Tlemcen. *Applied hydrogeology of the karst aquifers of the Tlemcen Mountains*, 1986, Avignon Thesis 272 p.

Dazy J., Dray M., Jusserand C., Pasqualotto M. & Zuppi G.-M. (1987). Caractérisation isotopique des eaux thermominérales des Alpes du Nord franco-italiennes. *Isotopic characterization of thermomineral waters from the French-Italian Northern Alps*, Proceedings Symposium IAEA-UNESCO, Vienna, 30 march-3 april 1987.

De Andrade E.-M., Queiroz Palácio H.-A., Souzai. H. & De Oliveira Leão M.-J.-G. (2008). *Land use effects in groundwater composition of an alluvial aquifer (Trussu River, Brazil) by multivariate techniques*, Environmental Research, 106, 2, February 2008, 170–177.

ENAGEO, ENTREPRISE NATIONALE DE GEOPHYSIQUE - Mission GA 263. (1979). Etude géophysique et hydrogéologique des Monts de Tlemcen. *Geophysical and hydrogeological study of the Tlemcen Mountains.*

ENAGEO, ENTREPRISE NATIONALE DE GEOPHYSIQUE - Mission HG 243 (DU 06/10/1983 AU 07/12/1983). Etude géophysique des régions à l'Ouest de Tlemcen et la Plaine d'Hennaya. *Geophysical study of the regions west of Tlemcen and the Hennaya Plain.*

ENAGEO, ENTREPRISE NATIONALE DE GEOPHYSIQUE. (1987). Prospection géophysique dans les Monts de Tlemcen. *Geophysical prospecting in the Tlemcen Mountains.*

Fekraoui A. (2007). Caractéristiques géochimiques des eaux géothermales de la région d'Oran. *Geochemical characteristics of the geothermal waters of the Oran region*, Renewable Energy Review CER'07. Oujda. 75-80.

Guardia P. (1984). Notice et Carte géologique Oranie nord occidentale à 1/100 000. *Geological Map North-West Orania at 1:100,000.* University of Nice

Gueddari H., Akodad M., Baghour M., Moumen A., Skalli A., El Yousfi Y., Ismail A., Chahban M., Azizi G., Ait Hmeid M. Z., (2022). The salinity origin and hydrogeochemical evolution of groundwater in the Oued Kert basin, northeastern of Morocco. Scientific African 16 (2022) e01226 http://creativecommons.org/licenses/by-nc-nd/4.0/

Hamit A. (2012). Étude du fonctionnement hydrogéochimique du système aquifère du Chari Baguirmi (République du Tchad). *Study of the hydrogeochemical functioning of the Chari Baguirmi aquifer system (Republic of Chad)*, Poitiers thesis. 319 p.

Helena B., Pardo R., Vega M., Barrado E., Fernandez J.-M. & Fernandez L. (2000). Temporal evolution of groundwater composition in an alluvial aquifer (Pisuerga River, Spain) by principal component analysis, Water Research, 34, 3, 15 February 2000, 807–816.

ICOSIUM forage et engineering services (2002). Prospection électrique dans la région de Remchi-Aïn Youcef et Hennaya" Wilaya de Tlemcen". *Electrical prospecting in the region of Remchi-Aïn Youcef and Hennaya" Wilaya of Tlemcen"*, Report of the National Agency for Hydraulic Resources, 26-31

Issaadi A. (1996). Mécanismes de fonctionnement des systèmes hydrothermaux. Application aux eaux thermominérales algériennes et aux eaux de Hammam Bou-Hadjar. *Mechanisms of operation of hydrothermal systems. Application to Algerian thermomineral waters and the waters of Hammam Bou-Hadjar*, Bulletin of the Geological Survey of Algeria 7, 1, 71-85.

Issaadi A. (2005). Identification et origine des gaz associes aux sources minérales, thermales et thermominérales algériennes. Apports à la connaissance de la géologie profonde de l'Algérie septentrionale. *Identification and origin of gases associated with Algerian mineral, thermal and thermomineral springs. Contributions to the knowledge of the deep geology of northern Algeria*, Bulletin of the Geological Survey of Algeria , 16, 2, 115 - 125.

Kedaid F. Z. (2006). Développement de la base de données géothermiques de l'Algérie par un système d'information géographique. *Development of Algeria's geothermal database by a geographic information system*, Revue des Energies Renouvelables, 9, 4, 253 – 258.

Kerzabi R. (2008). Identification de l'aquifère des grès serravalliens du bassin miocène dans la région de Remchi-Hennaya- Bensekrane et Ouled Mimoun. *Identification of the Serravallian sandstone aquifer of the Miocene basin in the region of Remchi-Hennaya-Bensekrane and Ouled Mimoun*, Magister of the University of Tlemcen, 87 p.

Khaska M., Le Gal La Salle C., Lancelot J., ASTER team, Mohamad A., Verdoux P., Noret A. & Simler R. (2013). Origin of groundwater salinity (current seawater vs. saline deep water) in a coastal karst, Applied Geochemistry, 37 212–227.

Lakrout, A., Meddah, B., & Ali Rahmani, S. E. (2022). Geochemical assessment of thermal water in Bouhanifia aquifer system: suitability for touristic therapeutic treatment. Applied Water Science, 12(8), 204.

Lloyd J.W. & Heathcoat J.A. (1985). Natural inorganic hydrochemistry in relation to groundwater: an introduction. Oxford University Press, New York, 296 p.

Mansour H., Nadji A. & Issaadi A. (2011). La tectonique récente et ses conséquences sur le thermominéralisme de Hammam Bou-Hadjar (Ain Témouchent, Algérie nord occidentale). *Recent tectonics and its consequences on the thermomineralism of Hammam Bou-Hadjar (Ain Témouchent, northwestern Algeria)*, Africa Geoscience Review, 18, 2, 93-10

Marín Celestino, A. E., Martínez Cruz, D. A., Otazo Sánchez, E. M., Gavi Reyes, F., & Vásquez Soto, D. (2018). Groundwater quality assessment: An improved approach to K-means clustering, principal component analysis and spatial analysis: A case study. Water, 10(4), 437.

Meddi M M, Arkamose A & Meddi H (2010). Temporal Variability of Annual Rainfall in the Macta and Tafna Catchments Northwestern Algeria. Water Resour Manage, v. 24, n. 2010 pp. 3817–3833. DOI 101007/s11269-010-9635-7.

Mhamdi, A., Moussaoui, I., Khalfi, C. Tarki M. & Dassi L. (2022). Assessment of groundwater mineralization processes in the Garâat Douza-Tebeddit shallow aquifer, Southwestern Tunisia: an integrated geoelectrical and hydrochemical approach. Carbonates Evaporites 37, 33. https://doi.org/10.1007/s13146-022-00781-6

Mouser P.-J., Rizzo D.-M., Röling W.-F.-M. & Breukelen M. (2005). A Multivariate Statistical Approach to Spatial Representation of Groundwater Contamination using Hydrochemistry and Microbial Community Profiles, Environmental Science and Technology, 39 (19), 7551–7559.

Mudry J. (1987). Apport du traçage physico-chimique naturel à la connaissance hydrocinématique des aquifères carbonatés. *Contribution of natural physico-chemical tracing to the hydrokinetic knowledge of carbonate aquifers*, Besançon thesis, 311p.

Nedjaï R. (1987). Etude hydrogéologique et hydrochimique des eaux thermales du centre algérien (Nord). *Hydrogeological and hydrochemical study of the thermal waters of central Algeria (North)*, Grenoble Thesis, 201 p

Ouali S., Khellaf A. & Baddari K. (2007). Etude des ressources géothermiques du sud algérien. *Study of geothermal resources in southern Algeria*, 2007, Revue des Energies Renouvelables , 10, 3, 407 – 414.

Razack M. & Dazy J. (1990). Hydrochemical characterization of groundwater mixing in sedimentary and metamorphic reservoirs with combined used of Piper's principle and factor analysis, Journal of Hydrology, 114, 371-393.

Rodier J. (2009). L'analyse de l'eau: Eaux naturelles, eaux résiduaires, eau de mer. *Water analysis: Natural waters, waste water*, seawater. 8th Edition Dunod..

Saberinasr, A., Morsali, M., Hashemnejad, A., & Hassanpour, J. (2019). Determining the origin of groundwater elements using hydrochemical data (case study: Kerman water conveyance tunnel). Environmental Earth Sciences, 78, 1-17.

Touati H. & Nebia R. (2019). Apport des SIG à la caractérisation hydrogéologique et hydrochimique des eaux souterraines des bassins versants d'Oued Zitoun-Oued Boumessaoud (Monts de Tlemcen, Nord-Ouest Algérie). *Contribution of GIS to the hydrogeological and hydrochemical characterization of groundwater in the watersheds of Oued Zitoun-Oued Boumessaoud (Tlemcen Mountains, North-West Algeria).* Master's thesis, University of Tlemcen, 92 p.

Telford, W. M., Geldart, L. P., & Sheriff, R. E. (1990). Applied geophysics. Cambridge university press.

Yebdri L. (2023). Etude de la vulnérabilité des eaux du bassin versant de la Tafna (Algérie, nord-occidentale). *Study of the vulnerability of the waters of the Tafna watershed (Algeria, north-west)*, Ph.D. Thesis in Science University of Tlemcen,, 230 p.

Yousfi S. (2014). Étude hydrodynamique et modélisation des écoulements souterrains dans les gouttières synclinales gréseuses du Barrémo-Albo-Aptien d'Aïn Séfra (partie centrale des Monts des Ksour – Atlas Saharien, Nord-Ouest Algérie). *Hydrodynamic study and modelling of groundwater flows in the sandstone synclinal gutters of the Barrémo-Albo-Aptien of Aïn Séfra (central part of the Ksour Mountains – Saharan Atlas, North-West Algeria)*, Ph.D. thesis Hydrogeology University of Oran and University of Franche-Comté.

Zamroni A., Sugarbo O., Trisnaning T. P., Sagala S. T. and Putra A. S. (2021). Geochemical Approach for Seawater Intrusion Assessment in the Area around Yogyakarta International Airport, Indonesia. Iraqi Geological Journal, 2021, 54 (1F), 1-11. DOI: 10.46717/igj.54.1F.1ms-2021-06-21